

# Genome-wide identification of the MADS-box gene family in *Avena sativa* and its role in photoperiod-insensitive oat

Jinsheng Nan<sup>1</sup>, Jianghong An<sup>1,2</sup>, Yan Yang<sup>1</sup>, Guo-fen Zhao<sup>1</sup>, Xiaohong Yang<sup>3</sup>, Hui-Yan Liu<sup>1</sup>, Bing Han<sup>Corresp. 1</sup>

<sup>1</sup> Inner Mongolia Agricultural University, Key Lab of Germplasm Innovation and Utilization of Triticeae Crop at Universities of Inner Mongolia Autonomous Region, Inner Mongolia Agricultural University, Hohhot, Inner Mongolia, China

<sup>2</sup> Inner Mongolia Academy of Agriculture and Animal Husbandry Science, Hohhot, Inner Mongolia, China

<sup>3</sup> Zhangjiakou Academy of Agricultural Sciences, Zhangjiakou, HeBei Province, China

Corresponding Author: Bing Han  
Email address: hb\_nmg@163.com

**Background.** Traditional spring-summer sown oat is a typical long-day crop that cannot head under short-day conditions. The creation of photoperiod-insensitive oats overcomes this limitation. MADS-box genes are a class of transcription factors involved in plant flowering signal transduction regulation. Previous transcriptome studies have shown that MADS-box genes may be related to the oat photoperiod. **Methods.** Putative MADS-box genes were identified in the whole genome of oat. Bioinformatics methods were used to analyze their classification, conserved motifs, gene structure, evolution, chromosome localization, collinearity and *cis*-elements. Ten representative genes were further screened via qRT-PCR analysis under short days. **Results.** In total, sixteen *AsMADS* genes were identified and grouped into 9 subfamilies. The domains, conserved motifs and gene structures of all *AsMADS* genes were conserved. All members contained light-responsive elements. Using the photoperiod-insensitive oat MENGSIYAN4HAO (MSY4) and spring-summer sown oat HONGQI2HAO (HQ2) as materials, qRT-PCR analysis was used to analyze the *AsMADS* gene at different panicle differentiation stages under short-day conditions. Compared with HQ2, *AsMADS3*, *AsMADS8*, *AsMADS11*, *AsMADS13*, and *AsMADS16* were upregulated from the initial stage to the branch differentiation stage in MSY4, while *AsMADS12* was downregulated. qRT-PCR analysis was also performed on the whole panicle differentiation stages in MSY4 under short-day conditions, the result showed that the expression levels of *AsMADS9* and *AsMADS11* gradually decreased. Based on the subfamily to which these genes belong, the above results indicated that *AsMADS* genes, especially SVP, SQUA and M $\alpha$  subfamily members, regulated panicle development in MSY4 by responding to short-days. This work provides a foundation for revealing the function of the *AsMADS* gene family in the oat photoperiod pathway.

1 **Genome-wide identification of the MADS-box gene family in *Avena sativa* and its**  
2 **role in photoperiod-insensitive oat**

3

4 Jin-sheng Nan<sup>1</sup>, Jiang-hong An<sup>1,2</sup>, Yan Yang<sup>1</sup>, Guo-fen Zhao<sup>1</sup>, Xiao-hong Yang<sup>3</sup>, Hui-yan Liu<sup>1</sup>,  
5 Bing Han<sup>1,\*</sup>

6 Key Lab of Germplasm Innovation and Utilization of Triticeae Crop at Universities of Inner Mongolia Autonomous Region

7 <sup>1</sup> Key Lab of Germplasm Innovation and Utilization of Triticeae Crop at Universities of Inner  
8 Mongolia Autonomous Region, Inner Mongolia Agricultural University, Hohhot, 010018, China

9 <sup>2</sup> Inner Mongolia Academy of Agricultural & Animal Husbandry Sciences, Hohhot, 010031,  
10 China

11 <sup>3</sup> Zhangjiakou Academy of Agricultural Sciences, Zhangjiakou, 075000, China

12

13 Corresponding Author:

14 Bing Han<sup>1</sup>

15 No. 306, Zhaowuda Road, Saihan District, Hohhot, Inner Mongolia, 010018, China.

16 Email address: hb\_nmg@163.com (B. Han)

17

18

19

20

21

22 **Abstract**

23 **Background.** Traditional spring-summer sown oat is a typical long-day crop that cannot head  
24 under short-day conditions. The creation of photoperiod-insensitive oats overcomes this  
25 limitation. MADS-box genes are a class of transcription factors involved in plant flowering  
26 signal transduction regulation. Previous transcriptome studies have shown that MADS-box genes  
27 may be related to the oat photoperiod.

28 **Methods.** Putative MADS-box genes were identified in the whole genome of oat. Bioinformatics  
29 methods were used to analyze their classification, conserved motifs, gene structure, evolution,  
30 chromosome localization, collinearity and *cis*-elements. Ten representative genes were further  
31 screened via qRT-PCR analysis under short days.

32 **Results.** In total, sixteen *AsMADS* genes were identified and grouped into 9 subfamilies. The  
33 domains, conserved motifs and gene structures of all *AsMADS* genes were conserved. All  
34 members contained light-responsive elements. Using the photoperiod-insensitive oat  
35 MENGSIYAN4HAO (MSY4) and spring-summer sown oat HONGQI2HAO (HQ2) as materials,  
36

37 qRT-PCR analysis was used to analyze the *AsMADS* gene at different panicle differentiation  
38 stages under short-day conditions. Compared with HQ2, *AsMADS3*, *AsMADS8*, *AsMADS11*,  
39 *AsMADS13*, and *AsMADS16* were upregulated from the initial stage to the branch differentiation  
40 stage in MSY4, while *AsMADS12* was downregulated. qRT-PCR analysis was also performed

41 on the whole panicle differentiation stages in MSY4 under short-day conditions, the result  
42 showed that the expression levels of *AsMADS9* and *AsMADS11* gradually decreased. Based on  
43 the subfamily to which these genes belong, the above results indicated that *AsMADS* genes,  
44 especially SVP, SQUA and M $\alpha$  subfamily members, regulated panicle development in MSY4 by  
45 responding to short-days. This work provides a foundation for revealing the function of the  
46 *AsMADS* gene family in the oat photoperiod pathway.

47

48 **Keywords.** *Avena sativa* L; MADS-box gene family; Photoperiod; Short-day; Gene expression

49

## 50 Introduction

51 Among the cereal crops, oat (*Avena sativa* L.) is cultivated worldwide as a food and forage crop.  
52 Traditional spring-summer sown oat is a long-day crop that cannot head without light in winter  
53 in the Northern Hemisphere (Yang et al., 2018). This traditional oat generally requires at least 14  
54 h of sunlight per day to head (An et al., 2018). This feature of oats limits the expansion of the oat  
55 growing area. New photoperiod-insensitive germplasm was bred by "Interspecific Polymer  
56 Crossing Methods" and could complete the entire growth period and set seeds in natural short-  
57 day conditions in HaiNan, China (11 h light/13 h dark) (Yang et al., 2014). The creation of this  
58 new oat germplasm overcame the previous limitations of photoperiod-sensitive oat. However,  
59 the reason why photoperiod-insensitive oats can complete the growth period under short days has  
60 not been elucidated. Transcriptome studies have been conducted previously on photoperiod-  
61 insensitive materials and traditional oats, revealing that MADS genes may be related to the  
62 photoperiod insensitivity of oat (An et al., 2020).

63 As transcriptional regulatory factors, MADS-box proteins play a key role in controlling the  
64 signal transduction processes of plant flowering time, flower organ formation and meristem  
65 specificity (Becker & Günter 2003). Hundreds of MADS-box genes have been found in many  
66 plants, such as Arabidopsis (Parenicová et al., 2003) maize (Zhao et al., 2011), rice (Arora et al.,  
67 2007), and wheat (Schilling et al., 2020). There are two types of MADS-box genes in plants,  
68 type I (SRF-like) and type II (MEF2-like, or MIKC type) (Smaczniak et al., 2012). Type I genes  
69 usually contain only one or two exons, with one highly conserved SRF-like MADS domain, and  
70 lack the K domain. Type II genes contain four conserved domain structures: the M domain  
71 (MADS-box), I domain (Intervening), K domain (Keratin-Like) and C-terminal domain  
72 (Henschel et al., 2002). Most of the MIKC-type MADS-box genes contain 6 introns and 7 exons,  
73 called MIKC<sup>C</sup>, while some contain 7 introns and 8 exons, called MIKC<sup>\*</sup>. In Arabidopsis, the type  
74 I MADS-box genes encode 3 types of proteins, including M $\alpha$ , M $\beta$  and M $\gamma$  types (Arora et al.,  
75 2007). The MIKC<sup>C</sup> proteins can be subdivided into 13 distinct subfamilies (AG, AGL6, AGL12,  
76 AGL15, AGL17, DEF/GLO, BS, FLC, SEP/AGL2, SQUA, SVP, TM3/SOC1 and AP3) (Theien  
77 2001). The MIKC<sup>\*</sup> type can be divided into the P type and S type. The P-type MIKC<sup>\*</sup> proteins  
78 identified in Arabidopsis are AGL30, AGL65 and AGL94, and the S-type proteins are AGL66,  
79 AGL67 and AGL104 (Michiel et al., 2012).

80 The ABCDE model is a classical genetic regulatory mechanism of flower organ development in  
81 Arabidopsis (Theien 2001). AP1 is an A-type gene whose functions include recognition genes

82 that promote the formation of floral meristems and the development of sepals, petals and other  
83 floral organs (Kempin et al., 1995). The AP1/SQUA homologous gene VRN1 in wheat is a  
84 flowering activator and is regularly expressed in leaves under long- and short-day conditions.  
85 VRN1 is located upstream of FT, upregulates FT expression and promotes flowering under long-  
86 day conditions (Shimada et al., 2009). DEF/GLO is a B-class gene that controls the morphology  
87 of the floral organs such as stamens and petals (Kai-Uwe et al., 2002). In Arabidopsis, the  
88 formation of sepals, petals, stamens, carpels and ovules is related to the SEP gene, which forms a  
89 MADS protein complex with A, B, C, and D proteins to work together in the morphogenesis of  
90 floral organs (Favaro et al., 2003). SVP-group MADS-box genes were first identified as  
91 flowering suppressor regulators in Arabidopsis. In rice, their roles in regulating meristem identity  
92 are well conserved, and their involvement in determining flowering time is not significant (Lee  
93 et al., 2008).

94 To explore their role in the photoperiod insensitivity of oat, the MADS-box gene family was  
95 identified at the genome-wide level. In this study, 16 MADS members were identified in *Avena*  
96 *sativa*, and their phylogenetic relationship, gene structure, conserved motifs, chromosome  
97 localization and collinearity were analyzed, along with *cis*-elements in the promoter region of all  
98 identified MADS-box genes. Transcriptome data conducted in the initial stage of oat panicle  
99 differentiation in the traditional oat HongQi2hao (HQ2) and photoperiod-insensitive oat MSY4  
100 under short days were used for differential expression analysis. In addition, the expression  
101 patterns of candidate genes at different panicle differentiation stages under short days were  
102 analyzed. Our results help to further reveal the biological function of MADS genes in  
103 photoperiod-insensitive oat and help to lay a foundation for revealing the mechanism of  
104 photoperiod insensitivity in oat.

105

## 106 **Materials & Methods**

### 107 **Identification of MADS genes in *Avena sativa* L.**

108 To identify the potential MADS-box genes in oat, the genome sequences were obtained from the  
109 GrainGenes database ([https://wheat.pw.usda.gov/GG3/graingenes\\_downloads/oat-ot3098](https://wheat.pw.usda.gov/GG3/graingenes_downloads/oat-ot3098)). The  
110 MADS-box protein sequences of Arabidopsis (<https://www.arabidopsis.org>) and rice  
111 (<http://rapdb.dna.affrc.go.jp/download/irgsp1.html>) were downloaded. Hidden Markov Model-  
112 based searches (<http://hmmer.janelia.org/>), built from these known MADS-box protein  
113 sequences, were used to search the MADS-box proteins in oat and as queries to search against  
114 the oat protein databases with the BLASTP program with an e-value of  $1 \times e^{-10}$  as the threshold.  
115 The software pfamscan and the PFAM A database were used to annotate the domains of the  
116 candidate *AsMADS* sequences, and the sequence containing the PF00319 domain was determined  
117 to be the final MADS-box sequence in oat. The information of sequence length, molecular  
118 weight, isoelectric points, and the instability index was obtained from the Expsay website  
119 (<http://web.expasy.org/protparam/>) (Panu et al., 2012). The subcellular localization was predicted  
120 using the Softberry website  
121 (<http://www.softberry.com/berry.phtml?topic=protcomppl&group=programs&subgroup=proloc>).

## 122 **Sequence alignment and phylogenetic analysis**

123 The MADS-box protein sequences of Arabidopsis (<https://www.arabidopsis.org>) and rice  
124 (<http://rapdb.dna.affrc.go.jp/download/irgsp1.html>) were downloaded and contained 108 and 75  
125 sequences, respectively. Sequence alignment and evolution analysis were carried out on the  
126 MADS protein sequences identified in oat, Arabidopsis and rice. Mafft  
127 (<https://omictools.com/mafft-tool>) was used for protein multiple sequence alignment. DNAMAN  
128 software was used to align sequences and recheck data result. Both NCBI batch CDD searches  
129 and pfamscan were used to double check the conserved domains. TBtools software  
130 (<http://www.tbtools.com/>) was used for visual display (Chen et al., 2020). MEGA version 7 was  
131 used for neighbor-joining (NJ) tree construction based on the alignment of MADS proteins  
132 (Sudhir et al., 2018). AsMADS genes were classified according to their phylogenetic  
133 relationships with the corresponding Arabidopsis (Parenicová et al., 2003) and rice (Arora et al.,  
134 2007) MADS genes.

## 135 **Gene structure, conserved motif analysis, Cis-element and protein structure analysis**

136 Gene structure prediction was performed in GSDS (<http://gsds.cbi.pku.edu.cn/>). The conserved  
137 motifs were analyzed by MEME software (<http://meme-suite.org/>) (Bailey et al., 2009). The  
138 upstream regulatory regions (2 kb from the translation start site) of *AsMADS* genes were  
139 obtained from the whole genome sequence of *Avena sativa* by TBtools. The *cis*-elements on the  
140 promoter were predicted by the website  
141 [http://plantregmap.cbi.pku.edu.cn/binding\\_site\\_prediction.php](http://plantregmap.cbi.pku.edu.cn/binding_site_prediction.php). The positions of the binding sites  
142 in the physical map of the gene promoters are marked and displayed. Protein secondary structure  
143 was investigated by the Prabi website ([https://npsa-prabi.ibcp.fr/cgi-](https://npsa-prabi.ibcp.fr/cgi-bin/npsa_automat.pl?page=npsa_sopma.html)  
144 [bin/npsa\\_automat.pl?page=npsa\\_sopma.html](https://npsa-prabi.ibcp.fr/cgi-bin/npsa_automat.pl?page=npsa_sopma.html)), and the 3D structure was predicted on the  
145 SWISS-MODEL website (<https://swissmodel.expasy.org/interactive>).

## 146 **Chromosome localization and collinearity analysis**

147 According to the position of *AsMADS* genes on the chromosome, the website  
148 [http://mg2c.iask.in/mg2c\\_v2.0/](http://mg2c.iask.in/mg2c_v2.0/) was used to draw the chromosome physical location map.  
149 MCSanX software was used to perform family gene collinearity analysis based on chromosome  
150 length information and gene structural annotation information. An intraspecific collinearity map  
151 of oat and an interspecific collinearity map of oat, rice and Arabidopsis were constructed.

## 152 **Transcriptional profile analysis**

153 For *AsMADS* gene expression analysis, RNA-seq data of *Avena sativa* L. materials with different  
154 photoperiod sensitivities under short-day conditions were obtained from previous laboratory data  
155 (An et al., 2020; Becker & Günter 2003). Short-day treatment-related transcriptome analysis was  
156 conducted in the initial stage of panicle development in that study, in which 10 MADS genes  
157 were differentially expressed in the panicles of HQ2 and MSY4. Heatmaps were generated using  
158 these data.

## 159 **Plant materials and treatments**

160 Similar to the materials used in the previous transcriptome study, MSY4 and HQ2 were used for  
161 specific expression analysis at different panicle developmental stages under short-days condition

162 (12 h). The seeding and shading methods were described in previous studies<sup>[1-3]</sup>. The young  
163 panicles, including those at the initial stage, elongation stage, spikelet differentiation stage, floret  
164 differentiation stage, pistil differentiation stage, and tetrad stage, were collected for expression  
165 analysis. Collected tissues were immediately frozen in liquid nitrogen and stored at -80°C until  
166 RNA isolation was performed.

#### 167 **Total RNA extraction and qRT-PCR expression analysis**

168 The total RNA of oat panicles was extracted using a TransZol Up Plus RNA Kit (Transgene,  
169 Beijing, China) and then reverse transcribed into cDNA by a TransScript® One-Step gDNA  
170 Removal and cDNA Synthesis Kit. The integrity of the RNA was analyzed by agarose gel  
171 electrophoresis, and the concentration and purity of the RNA were detected by a NanoDrop 2000.  
172 The cDNA was stored at -20°C for subsequent qRT-PCR. Specific primers for candidate genes  
173 in the MADS family were designed for qRT-PCR analysis using the Actin gene of oat as an  
174 internal reference gene (Yang et al., 2013). qRT-PCR was performed with SYBR-Green on a  
175 Jena Qtower 2.2 analyzer. According to the manufacturer's instructions, the 20 µL reaction  
176 contained 1 µL cDNA, 400 nM of each primer and 10 µL SYBR Green Mix. The amplification  
177 conditions were 95°C for 1 min and 40 cycles of 95°C for 10 s, 60°C for 10 s and 72°C for 10 s,  
178 with a melting curve over a temperature range of 60-95°C. Each experiment used three  
179 biological replicates and three technical replicates. The relative expression levels of genes were  
180 calculated using the  $2^{-\Delta\Delta C_t}$  method (Schmittgen 2008). Gene-specific DNA primers for qPCR  
181 are listed in supplementary file 7.

182

## 183 **Results**

### 184 **Identification and characterization of the MADS-box gene family in *Avena sativa* L.**

185 Based on the oat genome (OT3098), a total of 16 MADS-box genes with the PF00319 domain  
186 were identified through Hidden Markov Model, Blastp search and Pfam annotation, which were  
187 named *AsMADS1* to *AsMADS16*. Their basic properties were systematically evaluated, including  
188 gene ID and location, protein size, number of exons and introns, molecular weight, isoelectric  
189 points, instability index, GRAVY, and subcellular location (Table 1). The protein length of the  
190 *AsMADS* genes ranged from 142 to 278 amino acids, with 1 to 10 exons. The protein molecular  
191 weight ranged from 16.11 kDa (*AsMADS11*) to 31.61 kDa (*AsMADS2*), and the isoelectric points  
192 varied from 5.52 (*AsMADS3*) to 9.28 (*AsMADS16*). The hydrophobicity of the 16 proteins was  
193 negative. The instability index ranged from 44.82 to 65.59. The subcellular location prediction  
194 indicated that all members were located in the nucleus. The above results indicated that *AsMADS*  
195 genes were unstable hydrophobic nucleoproteins.

### 196 **Multiple sequence alignment and phylogenetic relationship analysis of MADS-box genes in** 197 ***Avena sativa* L.**

198 A multiple sequence alignment analysis of the 16 *AsMADS* proteins was conducted using mafft.  
199 The N-terminus of the sequence was conserved (Supplementary File 1). The 16 *AsMADS*  
200 protein sequences were analyzed for the presence of MADS-box and other domains using an  
201 NCBI batch CDD search. Our results showed that all the *AsMADS* proteins contained the M

202 domain, and 13 out of 16 AsMADS proteins contained the K domain, except for AsMADS4,  
203 AsMADS9, and AsMADS11 (Figure. 1). Moreover, 14 out of the 16 members belonged to type  
204 II MADS, and the remaining two (AsMADS9 and AsMADS11) belonged to type I MADS (Fig.  
205 1, Supplementary File 2 and 3).

206 To evaluate the evolutionary relationships among the AsMADS proteins, a phylogenetic tree was  
207 constructed using a bootstrapped neighbor-joining (NJ) method with the amino acid sequences of  
208 207 MADS genes (16 from oat, 108 from Arabidopsis, and 83 from rice). The phylogenetic  
209 analysis indicated that the 16 AsMADS members were grouped into 9 subfamilies: SEP/AGL2,  
210 AGL6, SQUA, AGL12, AG, BS, SVP, M $\alpha$ , and MIKC\* (Fig. 2). No members were grouped into  
211 the TM3/SOC1, AGL17, AGL15, FLC or M $\gamma$  subfamilies. The results showed that the SVP  
212 subfamily contained 3 AsMADS members, the SEP/AGL2, SQUA, AG, BS and M $\alpha$  subfamilies  
213 contained two members, and the remaining three subfamilies contained only one gene (Fig. 2,  
214 Supplementary File 3). In short, MADS genes in oats consisted of type I genes (*AsMADS9* and  
215 *AsMADS11*), MIKC\* (*AsMADS4*), and MIKC<sup>c</sup>-type genes (13 other AsMADS members).

### 216 **Structural analysis and conserved motif composition of the *AsMADS* gene family**

217 Gene structure prediction was performed in GSDS website, which showed that 15 *AsMADS*  
218 members contained multiple introns and exons, with the number of exons ranging from 5 to 10  
219 and the number of introns ranging from 4 to 9; *AsMADS9* only contained one exon (Table 1, Fig.  
220 3c). *AsMADS3*, *AsMADS8*, and *AsMADS13*, which were grouped in the SVP subfamily, had a  
221 similar intron/exon pattern, but *AsMADS9* and *AsMADS11* had radically different structures,  
222 even though they were grouped in the same subfamily.

223 The secondary structure of AsMADS proteins comprised an alpha helix, extended strand, beta  
224 turn, and random coil. The AsMADS proteins had a large proportion of alpha helix amino acids  
225 (>47%), followed by random coils (Supplementary File 4). The 3D structures of AsMADS  
226 proteins were predicted. Except for AsMADS11, 15 of the 16 AsMADS proteins had similar 3D  
227 structures (Fig. 4), indicating similar functions. 3D predicted structures of AsMADS11.  
228 Compared with other genes, it is clear that the 3D predicted structure of AsMADS11 contains  
229 less  $\alpha$ -helices and more  $\beta$ -sheets. This makes the 3D predicted structure of AsMADS11 look  
230 simpler. However, the secondary structural pattern of AsMADS11 was similar to that of the  
231 other members (Supplementary File 4).

232 The full-length protein sequences of 16 AsMADS were used to investigate the conserved motifs.  
233 In total, 15 different motifs were identified, and motifs 1, 2, 3 and 5 were widely distributed,  
234 indicating that they might be more conserved. Interestingly, motif 11 only existed in the BS  
235 subfamily (*AsMADS7* and *AsMADS15*), which may be related to its evolutionary history (Fig. 3b,  
236 Supplementary File 3).

### 237 **Chromosome localization and collinearity analysis of *AsMADS* genes**

238 Chromosomal distribution of the *AsMADS* gene family was visualized using TBtools and the oat  
239 genome annotation information. The 16 *AsMADS* genes were located on chromosomes 1D, 2D,  
240 3D, 4D, 6D, 7D, 1A, 3A, 6A, 7A, 2C and 6C (Table 1). Briefly, chromosomes 1D, 2C, 3A, and  
241 4D harbored 2 *AsMADS* genes, whereas the other chromosomes possessed only one *AsMADS*

242 gene. Additionally, most members were located on the ends of the chromosome, except for  
243 *AsMADS8* and *AsMADS10* (Fig. 5a).

244 The intraspecific and interspecific collinearity of MADS-box genes was visualized using  
245 TBTools. There was no collinearity among the 16 *AsMADS* genes on the oat chromosomes. The  
246 interspecific collinearity analysis among Arabidopsis, rice and oat showed that there were 16  
247 pairs of collinear genes between oat and rice, and one gene was syntenic among oat (*AsMADS2*),  
248 rice (Os01g10504.1) and Arabidopsis (AT4G18960), which was annotated as AG (Fig. 5b). The  
249 results showed that there was a high degree of conservation and consistency in the linear  
250 relationship of MADS-box gene evolution between oat and rice.

#### 251 **Prediction of *cis*-elements in the promoters of *AsMADS* genes**

252 The 2 kb upstream region of the *AsMADS* genes was extracted by TBtools, and submitted to the  
253 online website plantregmap to search for *cis*-elements. The top 12 putative *cis*-elements in the  
254 *AsMADS* promoters are shown (Fig. 6). In addition to typical promoter elements, such as TATA  
255 boxes and CAAT boxes, G-box, circadian, MYB, MYC, STRE, ABRE, as-1, CGTCA-motif and  
256 TGCAG-motif elements were predicted. The promoters of five *AsMADS* members contained  
257 circadian elements, namely, *AsMADS1*, *AsMADS7*, *AsMADS8*, *AsMADS11* and *AsMADS15*.  
258 Fourteen of the 16 members contained the light-responsive element G-box, except *AsMADS9*  
259 and *AsMADS15*, but *AsMADS9* contained other light-responsive elements, such as the I-box and  
260 sp1 (Supplementary File 5). These results indicated that the promoters of all *AsMADS* members  
261 contained light-responsive *cis*-acting elements.

#### 262 **GO enrichment and transcriptome expression analysis of *AsMADS* genes**

263 For the GO classification, the 16 *AsMADS* genes were categorized into three main categories:  
264 biological processes, cellular components and molecular functions (Fig. 7). *AsMADS* genes  
265 categorized as flower development (GO:0009908), floral meristem determinacy (GO:0010582),  
266 floral whorl structural organization (GO:0048459), floral organ formation (GO:0048449), and  
267 rhythmic process may be related to the photoperiod insensitivity of oat (Supplementary File 6).  
268 Based on previous transcriptome data from oat, a heatmap of the *AsMADS* gene expression  
269 levels at the initial stage of oat panicle differentiation in HQ2 and MSY4 under short days was  
270 drawn. Ten of 16 *AsMADS* members were differentially expressed in the transcriptome data. No  
271 matter in panicles or leaves, *AsMADS2*, *AsMADS11*, and *AsMADS16* were upregulated in MSY4,  
272 and *AsMADS3* and *AsMADS12* were downregulated in MSY4 (Fig. 8).

#### 273 **Expression analysis of *AsMADS* genes in HQ2 and MSY4 under short-day conditions**

274 In order to explore the expression specificity, the expression of *AsMADS* gene among materials  
275 with different photoperiod sensitivities was carried out. In HQ2, the panicle can only develop to  
276 the branch differentiation stage under short days, whereas in MSY4, it can complete the whole  
277 panicle differentiation process (An et al., 2018). Gene expression data for qPCR are listed in  
278 supplementary file 8. The expression levels of MSY4 and HQ2 were compared in the first three  
279 panicle differentiation stages. Compared with HQ2, *AsMADS3*, *AsMADS8*, *AsMADS11*,  
280 *AsMADS13*, and *AsMADS16* were upregulated at these three differentiation stages in MSY4,  
281 while *AsMADS12* was downregulated. *AsMADS6* and *AsMADS9* were downregulated in the

282 initial stage and elongation stage and then upregulated in the branch differentiation stage in  
283 MSY4 than in HQ2, while *AsMADS2* was downregulated in the initial stage and showed  
284 increased expression in the following two stages. The *AsMADS15* expression level remained  
285 basically unchanged throughout the panicle differentiation process between MSY4 and HQ2.  
286 With the development of the panicle in HQ2, the expression levels of the *AsMADS3*, *AsMADS8*,  
287 *AsMADS12* and *AsMADS13* genes gradually decreased (Fig. 9).  
288 In order to study the expression profile of *AsMADS* genes in MSY4 under short-day conditions  
289 during the entire panicle differentiation stages, real-time fluorescence quantitative analysis was  
290 carried out. With the development of the panicle in MSY4, the expression levels of the  
291 *AsMADS9* and *AsMADS11* genes gradually decreased. The expression levels of *AsMADS15* and  
292 *AsMADS16* were basically unchanged. The expression levels of the other six members fluctuated  
293 at different stages of panicle differentiation (Fig. 10).

294

295

## 296 Discussion

297 Oat is a long-day crop, which limits the expansion of its growing area. Using traditional breeding  
298 methods to change the photoperiod sensitivity of oats makes it possible to expand the oat  
299 planting area, accelerate the breeding rate, and increase the yield of oats. To date, photoperiod-  
300 insensitive oats have been created, but the underlying mechanism is unclear. Based on a previous  
301 transcriptome study (An et al., 2020), many candidate genes were found, so we focused on  
302 *MADS* genes due to their function in flower development and expression differences in  
303 transcriptome data.

304 The release of oat genome data will allow us to identify the *MADS* family at the genome level.  
305 Sixteen members were identified (Table 1) and classified into 9 subfamilies (Fig. 2), including  
306 the A-type, C/D-type and E-type genes in the ABCDE model. AP1/SQUA-like (A-type) genes  
307 can promote the formation of floral meristems (Ferrándiz et al., 2000). *OsMADS14* and  
308 *OsMADS18* are AP1/SQUA-like genes in rice. Overexpression of *OsMADS14* can shorten the  
309 heading period of rice and affect the formation of floral meristems, and overexpression of  
310 *OsMADS18* can cause early flowering (Jeon et al., 2000). The E-type usually forms *MADS*-box  
311 protein complexes with A-, B-, C- and D-type proteins to work together to affect floral organ  
312 morphology (Favaro et al., 2003). A total of 4 E genes (*SEP1/2/3/4*) were identified in  
313 Arabidopsis, and 5 SEP genes, namely, *OsMADS1*, *OsMADS5*, *OsMADS24*, *OsMADS34* and  
314 *OsMADS45*, were identified in rice (Pelucchi et al., 2002). *OsMADS1* is the most detailed SEP-  
315 like gene, and it plays a key role in the morphogenesis of floral organs (Prasad et al., 2001). The  
316 SVP gene controls flowering time in most dicot plants and is an inhibitor of flowering  
317 (Hartmann et al., 2000). However, the expression levels of *AsMADS8* and *AsMADS9* in the first  
318 seven stages of panicle development were also significantly higher than those of other *AsMADS*  
319 genes (Fig. 10). All of results indicated that SVP genes promoted the process of panicle  
320 development in MSY4 under short-day conditions.

321 Among relative species of oat, the numbers of *MADS* gene family members in wheat, barley,  
322 foxtail millet, maize and brachypodium were 300 (Q et al., 2021), 34 (HNJ et al., 2021), 89 (D et  
323 al., 2022), 211 (D et al., 2021) and 57 (B et al., 2014), respectively. The expansion and  
324 contraction of gene families is the result of the interaction between the plant and the external  
325 environment. The reason why the number of *MADS* genes in oats is less than that in other  
326 species may be the result of selection of this gene family during the evolution of oats, or the  
327 phenomenon of expansion in other species. The specific reasons need to be further studied.  
328 Plant *MADS* proteins were conserved (HNJ et al., 2021; O et al., 2010; R et al., 2002), and  
329 *MADS* proteins of oat were also conserved according to the intron/exon pattern, motif  
330 components and predicted 3D structures, type II (Fig. 3-4). *AsMADS9* and *AsMADS11* are type I  
331 *MADS* genes, and their gene structures are completely different. *AsMADS9* contains only 1 exon  
332 and no introns, while *AsMADS9* has 5 exons and a very long intron (Table 1, Fig. 3). Analysis of  
333 *cis*-elements revealed that all *AsMADS* genes contained light-responsive elements (Fig. 6).  
334 Therefore, the expression of *AsMADS* genes may be activated or inhibited by short-day  
335 conditions during panicle development in oats. Non-vernalized spring wheat grown under a  
336 short-day photoperiod accumulates VEGETATIVE TO REPRODUCTIVE TRANSITION 2  
337 (*TaVRT2*) and shows a delay in flowering, suggesting that *TaVRT2* is regulated independently  
338 by photoperiod (NA et al., 2007). *GmAGL1* was much more effective at promoting flowering  
339 under long-day conditions than under short-day conditions and *GmAGL1* overexpression not  
340 only resulted in early maturation but also promoted flowering and affected petal development (X  
341 et al., 2018). We found that the expression levels of the *AsMADS3*, *AsMADS12*, and *AsMADS13*  
342 genes gradually decreased with the development of the panicle in HQ2, and the expression levels  
343 of *AsMADS3*, *AsMADS11* and *AsMADS13* were higher in MSY4 than in HQ2. The expression  
344 levels of *AsMADS6*, *AsMADS8*, *AsMADS12*, and *AsMADS13* fluctuated with panicle  
345 development. *AsMADS2*, *AsMADS8*, *AsMADS12* and *AsMADS16* belonged to the AG, SVP and  
346 SQUA subfamilies. The main genes that promote MSY4 panicle development under short-day  
347 conditions may be SVP, SQUA and *Mα* genes. In short, high expression of *AsMADS* genes in  
348 MSY4 promoted panicle development, while low expression in HQ2 resulted in the arrest of  
349 panicle development.

350 Combined with previous transcriptome studies, the photoperiod pathway of MSY4 in response to  
351 short days was predicted. After the seedlings were unearthed, the expression of photoreceptors  
352 changed upon sensing inductive sunlight conditions (Makoto Takano et al., 2005). The  
353 expression of *PhyB* increased, and the expression of *PhyC* and *Cry1* decreased. Photoreceptors  
354 transmit light signals to circadian genes. The expression levels of *CCA1* and *PRR* genes both  
355 decreased. The expression of *GI* decreased, as it is regulated by the circadian clock and can  
356 affect the magnitude of circadian rhythm changes. The expression of *CO* in the phloem activates  
357 the flower-flowering pathway integration gene *FT* and initiates plant flowering. However, *FT*  
358 was not differentially expressed in the initial stage. The factor that actually causes MSY4 to  
359 flower under short-day conditions may lie in the process of floral meristem determination. The  
360 *FT* protein is transported from the leaf to the apical meristem cytoplasm to interact with the 14-3-

361 3 protein and then enters the nucleus together with the transcription factor FD protein to form the  
362 florigen activation complex and activate the downstream floral meristem genes (Ken-ichiro  
363 Taoka 2011). The MADS-box plays an important regulatory role in the developmental process of  
364 determining the characteristics of floral meristems. In this study, multiple MADS-box genes  
365 were detected to be highly expressed in the panicles of MSY4. In particular, the high expression  
366 of the MADS-box genes in the SVP, SQUA and M $\alpha$  subfamilies regulate the heading and  
367 flowering of MSY4 under short-day conditions (Fig. 11).

368

### 369 **Conclusions**

370 In this study, 16 *AsMADS* genes were identified from the oat genome and could be divided into 9  
371 subfamilies. The structures of *AsMADS* members were relatively conserved, but there was no  
372 collinearity among them. All members contained light-responsive elements and their expression  
373 levels were regulated by light. The expression profiles indicated that *AsMADS* genes belonging  
374 to the SVP, SQUA and M $\alpha$  subfamilies mainly regulate the panicle differentiation process of  
375 MSY4 under short-day conditions. Our results can be used for the further functional analysis of  
376 these *AsMADS* genes in the photoperiod response under short days.

377

### 378 **Acknowledgments**

379 We thank the China National Germplasm Bank for providing the photoperiod-insensitive  
380 material MSY4.

381

382

### 383 **References**

- 384 An Jianghong, Rong Xiaoping, Yang Xiaohong, Li Tianliang, Zhang Ruixia, Han Bing, and Yang  
385 Cai. 2018. Response of new oat germplasm to different lengths of sunlight hours.  
386 *JOURNAL OF NORTHERN AGRICULTURE* 46:1-8. DOI: 10.3969/j.issn.2096-  
387 1197.2018.06.01
- 388 An Jianghong, Yu Dongyang, Yang Xiaohong, Rong Xiaoping, Han Bing, Yang Cai, Yang Yan,  
389 Zhou Haitao, and Li Tianliang. 2020. Combined transcriptome sequencing reveals the  
390 photoperiod insensitivity mechanism of oats. *Plant Physiology and Biochemistry*  
391 146:133-142. DOI: 10.1016/j.plaphy.2019.11.015
- 392 Arora R., Agarwal P., Ray S., Singh A. K., Singh V. P., Tyagi A. K., and Kapoor S. 2007. MADS-  
393 box gene family in rice: genome-wide identification, organization and expression profiling  
394 during reproductive development and stress. *Bmc Genomics* 8:242. DOI: 10.1186/1471-  
395 2164-8-242
- 396 B Wei, RZ Zhang, JJ Guo, DM Liu, AL Li, RC Fan, L Mao, and XQ Zhang. 2014. Genome-wide  
397 analysis of the MADS-box gene family in *Brachypodium distachyon*. *Plos One* 9:e84781.  
398 10.1371/journal.pone.0084781
- 399 Bailey Timothy L, Mikael Boden, Buske Fabian A, Martin Frith, Grant Charles E, Luca Clementi,  
400 Jingyuan Ren, Li Wilfred W, and Noble William S. 2009. MEME SUITE: tools for motif  
401 discovery and searching. *Nucleic Acids Research* 37:W202-208. DOI:  
402 10.1093/nar/gkp335
- 403 Becker Annette, and Günter Theissen. 2003. The major clades of MADS-box genes and their  
404 role in the development and evolution of flowering plants. *Molecular Phylogenetics and*  
405 *Evolution* 29:464-489. DOI: 10.1016/S1055-7903(03)00207-0

- 406 Chen C., Chen H., Zhang Y, Thomas H. R., and Xia R. 2020. TBtools: An Integrative Toolkit  
407 Developed for Interactive Analyses of Big Biological Data. *Molecular Plant* 13:1194-  
408 1202. DOI: 10.1016/j.molp.2020.06.009
- 409 D Lai, J Yan, A He, G Xue, H Yang, L Feng, X Wei, L Li, D Xiang, J Ruan, Y Fan, and J Cheng.  
410 2022. Genome-wide identification, phylogenetic and expression pattern analysis of  
411 MADS-box family genes in foxtail millet (*Setaria italica*). *Scientific reports* 12:4979.  
412 10.1038/s41598-022-07103-9
- 413 D Zhao, Z Chen, L Xu, L Zhang, and Q Zou. 2021. Genome-Wide Analysis of the MADS-Box  
414 Gene Family in Maize: Gene Structure, Evolution, and Relationships. *Genes* 12.  
415 10.3390/genes12121956
- 416 Favaro Rebecca, Pinyopich Anusak, Battaglia Raffaella, Kooiker Maarten, Borghi Lorenzo, Ditta  
417 Gary, Yanofsky Martin F., Kater Martin M., and Colombo Lucia. 2003. MADS-Box  
418 Protein Complexes Control Carpel and Ovule Development in Arabidopsis. *Plant Cell*  
419 15:2603-2611. DOI: 10.1105/tpc.015123
- 420 Ferrándiz C, Gu Q., Martienssen R., and Yanofsky M. F. 2000. Redundant regulation of  
421 meristem identity and plant architecture by FRUITFULL, APETALA1 and  
422 CAULIFLOWER. *Development* 127:725-734. DOI: 10.1007/PL00008234
- 423 Hartmann U., Hhmann S., Nettesheim K., Wisman E., Saedler H., and Huijser P. 2000.  
424 Molecular cloning of SVP: a negative regulator of the floral transition in Arabidopsis. *The*  
425 *Plant journal: for cell and molecular biology* 21:351-360. DOI: 10.1046/j.1365-  
426 313x.2000.00682.x
- 427 Henschel K., Kofuji R., Hasebe M., Saedler H., Munster T., Thei?En G., and Evolution. 2002.  
428 Two Ancient Classes of MIKC-type MADS-box Genes are Present in the Moss  
429 *Physcomitrella patens*. *Molecular Biology and Evolution* 19:801-814. DOI:  
430 10.1093/oxfordjournals.molbev.a004137
- 431 HNJ Kuijter, NJ Shirley, SF Khor, J Shi, J Schwerdt, D Zhang, G Li, and RA Burton. 2021.  
432 Transcript Profiling of MIKCC MADS-Box Genes Reveals Conserved and Novel Roles in  
433 Barley Inflorescence Development. *Frontiers in Plant Science* 12:705286.  
434 10.3389/fpls.2021.705286
- 435 Jeon J. S., Lee S., Jung K. H., Yang W. S., Yi G. H., Oh B. G., and An G. 2000. Production of  
436 transgenic rice plants showing reduced heading date and plant height by ectopic  
437 expression of rice MADS-box genes. *Molecular Breeding* 6:581-592. DOI:  
438 10.1023/A:1011388620872
- 439 Kai-Uwe Winter, Christof W., Kerstin K., Arend B., Charlotte K., Akira K., Heinz S., Günter T,  
440 and Evolution. 2002. Evolution of class B floral homeotic proteins: obligate  
441 heterodimerization originated from homodimerization. *Molecular Biology and*  
442 *Evolution*:587-596. DOI: 10.1097/00004872-200018030-00002
- 443 Kempin S. A., Savidge B., and Yanofsky M. F. 1995. Molecular basis of the cauliflower  
444 phenotype in Arabidopsis. *Science* 267:522-525. DOI: 10.1126/science.7824951
- 445 Ken-ichiro Taoka Izuru Ohki, Hiroyuki Tsuji, Kyoko Furuita, Kokoro Hayashi, Tomoko Yanase,  
446 Midori Yamaguchi, Chika Nakashima, Yekti Asih Purwestri, Shojiro Tamaki, Yuka Ogaki,  
447 Chihiro Shimada, Atsushi Nakagawa, Chojiro Kojima & Ko Shimamoto. 2011. 14-3-3  
448 proteins act as intracellular receptors for rice Hd3a florigen. *Nature Protocols* 476:332-  
449 335. DOI: 10.1038/nature10272
- 450 Lee S., Jeong D. H., and An G. 2008. A possible working mechanism for rice SVP-group  
451 MADS-box proteins as negative regulators of brassinosteroid responses. *Plant signaling*  
452 *& behavior* 3:471-474. DOI: 10.4161/psb.3.7.5677
- 453 Makoto Takano, Noritoshi Inagaki, Xianzhi Xie, Natsu Yuzurihara, Fukiko Hihara, Toru Ishizuka,  
454 Masahiro Yano, Minoru Nishimura, Akio Miyao, Hirohiko Hirochika, and Shinomura  
455 Tomoko. 2005. Distinct and cooperative functions of phytochromes A, B, and C in the

- 456 control of deetiolation and flowering in rice. *Plant Cell* 17:3311. DOI:  
457 10.1105/tpc.105.035899
- 458 Michiel Kwantes, Daniela Liebsch, and Wim Verelst. 2012. How MIKC\* MADS-Box Genes  
459 Originated and Evidence for Their Conserved Function Throughout the Evolution of  
460 Vascular Plant Gametophytes. *Molecular Biology and Evolution*:293-302. DOI:  
461 10.1093/molbev/msr200
- 462 NA Kane, Z Agharbaoui, AO Diallo, H Adam, Y Tominaga, F Ouellet, cell Sarhan F %J The  
463 Plant journal : for, and biology molecular. 2007. TaVRT2 represses transcription of the  
464 wheat vernalization gene TaVRN1. 51:670-680. 10.1111/j.1365-313X.2007.03172.x
- 465 O Zobell, W Faigl, H Saedler, biology Münster T %J Molecular, and evolution. 2010. MIKC\*  
466 MADS-box proteins: conserved regulators of the gametophytic generation of land plants.  
467 27:1201-1211. 10.1093/molbev/msq005
- 468 Panu A., Manohar J., Konstantin A., Delphine B., Gabor C., Edouard De Castro, Séverine D,  
469 Volker F., Arnaud F., and Elisabeth G. 2012. ExpASy: SIB bioinformatics resource  
470 portal. *Nucleic Acids Research*:W597-W603. DOI: 10.1093/nar/gks400
- 471 Parenicová L, Folter S. D., Kieffer M., Horner D. S., and Colombo L. 2003. Molecular and  
472 Phylogenetic Analyses of the Complete MADS-Box Transcription Factor Family in  
473 Arabidopsis New Openings to the MADS World. *The Plant Cell* 15:1538-1551. DOI:  
474 10.1353/hub.2002.0011
- 475 Pelucchi Nilla, Fornara Fabio, Favalli Cristina, Masiero Simona, Lago Clara, Pè Enrico M,  
476 Colombo Lucia, and Kater Martin M. 2002. Comparative analysis of rice MADS-box  
477 genes expressed during flower development. *Sexual Plant Reproduction* 15:113-122.  
478 DOI: 10.1007/s00497-002-0151-7
- 479 Prasad K., Sriram P., Kumar S. C., Kushalappa K., and Vijayraghavan U. 2001. Ectopic  
480 expression of rice OsMADS1 reveals a role in specifying the lemma and palea, grass  
481 floral organs analogous to sepals. *Development Genes Evolution* 211:281-290. DOI:  
482 10.1007/s004270100153
- 483 Q Raza, A Riaz, RM Atif, B Hussain, IA Rana, Z Ali, H Budak, and IA Alaraidh. 2021. Genome-  
484 Wide Diversity of MADS-Box Genes in Bread Wheat is Associated with its Rapid Global  
485 Adaptability. *Frontiers in genetics* 12:818880. 10.3389/fgene.2021.818880
- 486 R Favaro, RG Immink, V Ferioli, B Bernasconi, M Byzova, GC Angenent, M Kater, L Colombo,  
487 and MGG genomics : 2002. Ovule-specific MADS-box proteins have conserved protein-  
488 protein interactions in monocot and dicot plants. *Molecular Genetics and Genomics*  
489 268:152-159. 10.1007/s00438-002-0746-6
- 490 Schilling S., Kennedy A., Pan S., Jermiin L. S., and Melzer R. 2020. Genome - wide analysis of  
491 MIKC - type MADS - box genes in wheat: pervasive duplications, functional  
492 conservation and putative neofunctionalization. *New Phytologist* 225:511-529. DOI:  
493 info:doi/10.1111/nph.16122
- 494 Schmittgen Thomas D. 2008. Analyzing Real-time PCR data by the comparative CT method.  
495 *Nature Protocols* 3:1101-1108. DOI: 10.1038/nprot.2008.73>
- 496 Shimada S., Ogawa T., Kitagawa S., Suzuki T., Ikari C., Shitsukawa N., Abe T., Kawahigashi  
497 H., Kikuchi R., and Handa H. 2009. A genetic network of flowering-time genes in wheat  
498 leaves, in which an APETALA1/FRUITFULL-like gene, VRN1, is upstream of  
499 FLOWERING LOCUS T. *Plant Journal* 58:668-681. DOI: 10.1111/j.1365-  
500 313X.2009.03806.x
- 501 Smaczniak C., Immink Rgh, Angenent G. C., and Kaufmann K. 2012. Developmental and  
502 evolutionary diversity of plant MADS-domain factors: Insights from recent studies.  
503 *Development* 139:3081-3098. DOI: 10.1242/dev.074674

- 504 Sudhir K., Glen S., Li M., Christina K., and Koichiro T. 2018. MEGA X: Molecular Evolutionary  
505 Genetics Analysis across computing platforms. *Molecular Biology Evolution* 35:1547-  
506 1549. DOI: 10.1093/molbev/msy096
- 507 Theien Günter. 2001. Development of floral organ identity: Stories from the MADS house.  
508 *Current Opinion in Plant Biology* 4:75-85. DOI: 10.1016/S1369-5266(00)00139-4
- 509 X Zeng, H Liu, H Du, S Wang, W Yang, Y Chi, J Wang, F Huang, and genomics Yu D %J BMC.  
510 2018. Soybean MADS-box gene GmAGL1 promotes flowering via the photoperiod  
511 pathway. 19:51. 10.1186/s12864-017-4402-2
- 512 Yang Cai, Zhou Haitao, Li Tianliang, Zhang Xinjun, Yang Xiaohong, Liu Wenting, and Bai Jing.  
513 2014. The Breeding of Many Types of Oats Germplasm Resources Which Not Sensitive  
514 to Long Photoperiod Through Interspecific Polymer Crossing. *Seed* 33:4. DOI:  
515 10.16590/j.cnki.1001-4705.2014.04.062
- 516 Yang T., Sun S. S., Gao S. Q., Tang Y. M., and Zhao C. P. 2013. Cloning of AsRBP1 Gene  
517 from Oat(*Avena sterilis*) and Analysis on Its Expressions to Stresses. *Journal of Triticeae*  
518 *Crops* 33:217-223.
- 519 Yang Xiaohong, An Jianghong, Han Bing, Zhou Hai Tao, and Yang Cai. 2018. Effect of  
520 Simulated Short-day on Spike Development of Spring and Summer Sown Oat by  
521 Shading. *Biotechnology Bulletin* 34:93-97. DOI: 10.13560/j.cnki.biotech.bull.1985.2017-  
522 0741
- 523 Zhao Y., Li X., Chen W., Peng X., Xiao C., Zhu S., and Cheng B. . 2011. Whole-genome survey  
524 and characterization of MADS-box gene family in maize and sorghum. *Plant Cell Tiss*  
525 *Organ Cult* 105:159-173. DOI: 10.1007/s11240-010-9848-8  
526

# Figure 1

Conserved domain structure of 16 AsMADS proteins in *Avena sativa* L.

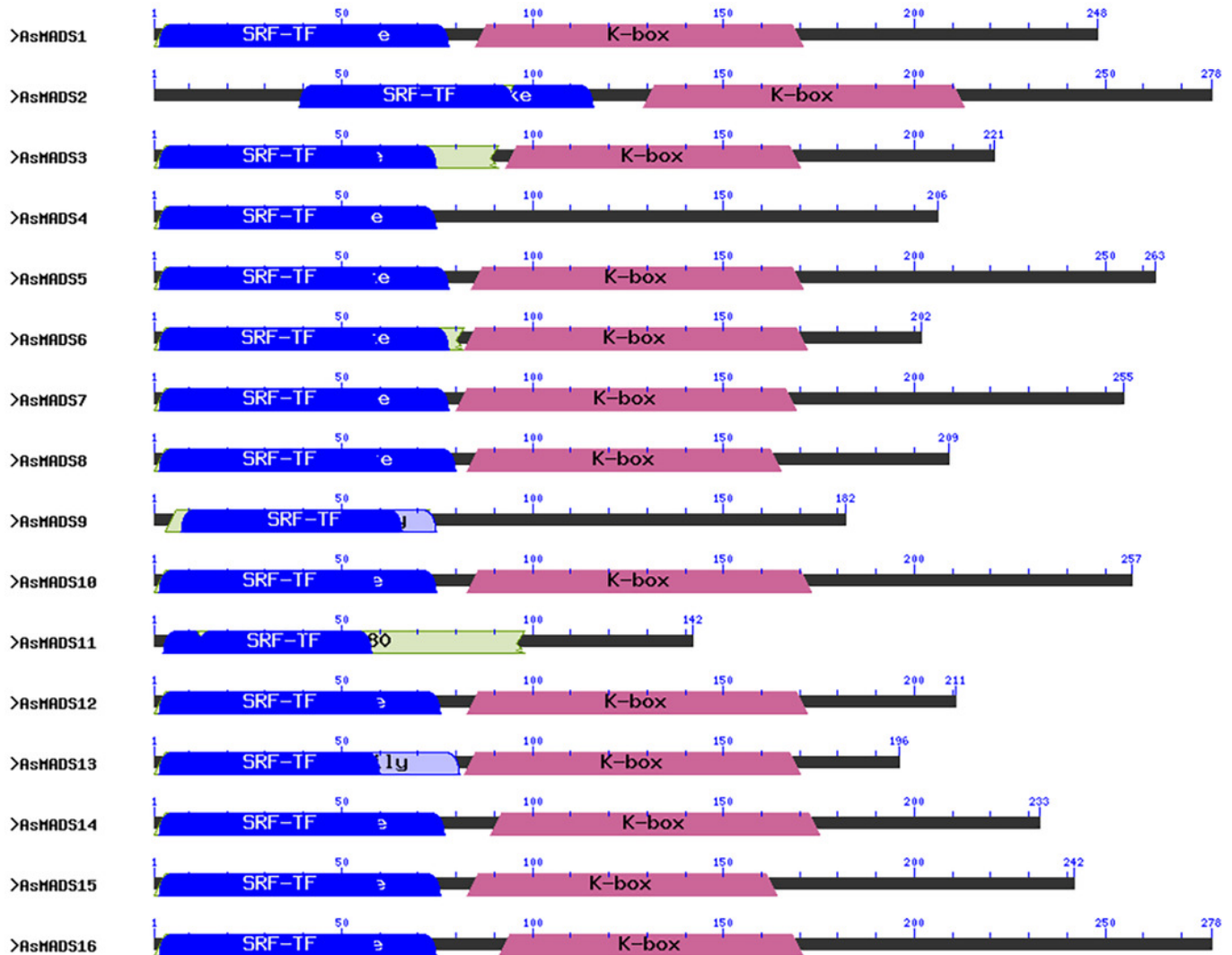


## Figure 2

A phylogenetic tree of the AsMADS gene family.

The MADS proteins of oat, Arabidopsis, and rice were clustered into 14 groups. Members of different colors belong to different groups.

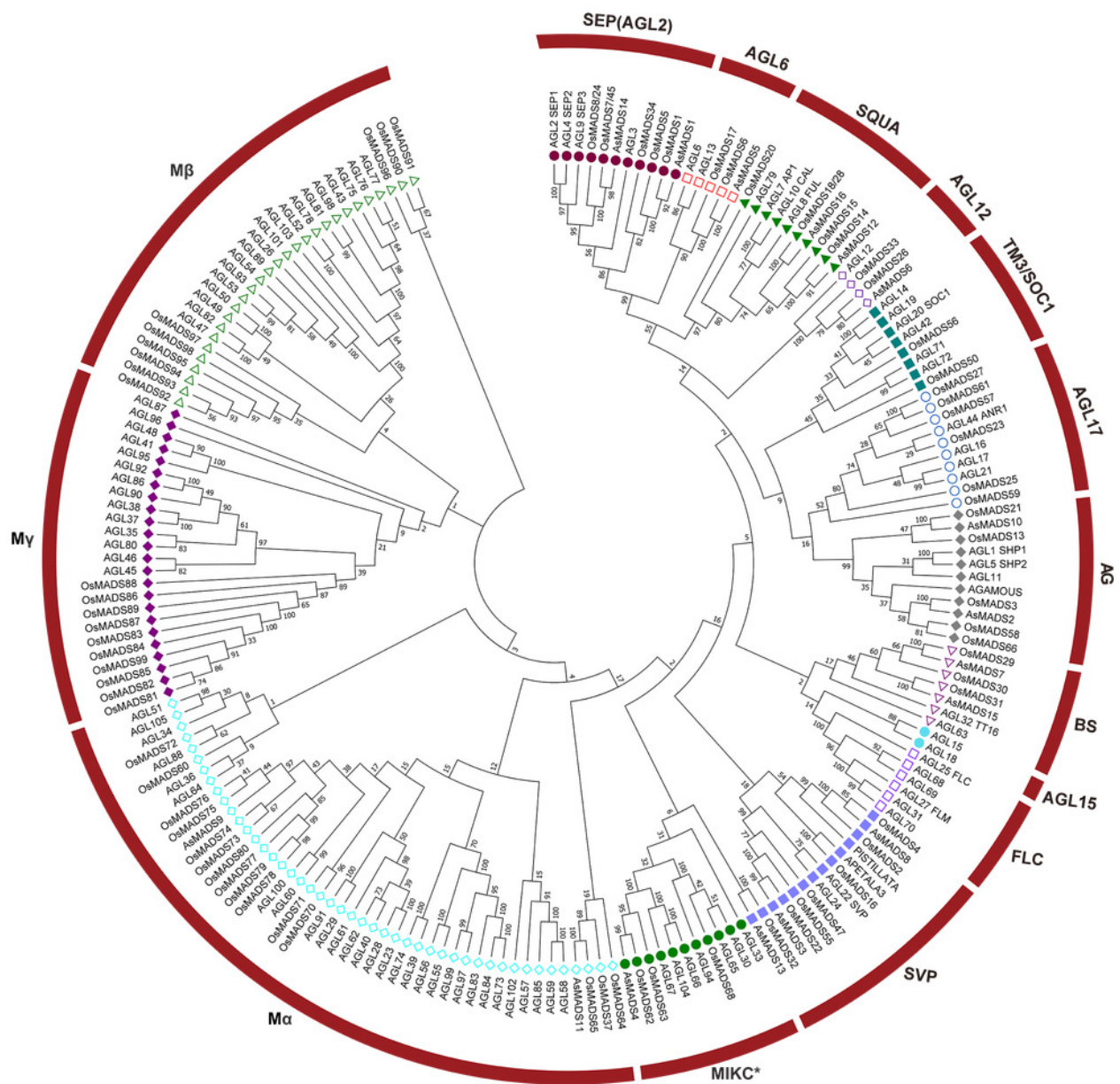


## Figure 3

Gene structure and architecture of conserved protein motifs in AsMADSs.

(a) The phylogenetic tree was constructed based on the full-length sequences of oat MADS family proteins using MEGA-7 software. (b) The motif compositions of AsMADSs. Different colored boxes display different motifs. (c) The exon-intron structure of AsMADSs. Yellow lines indicate CDSs, and black lines indicate introns.

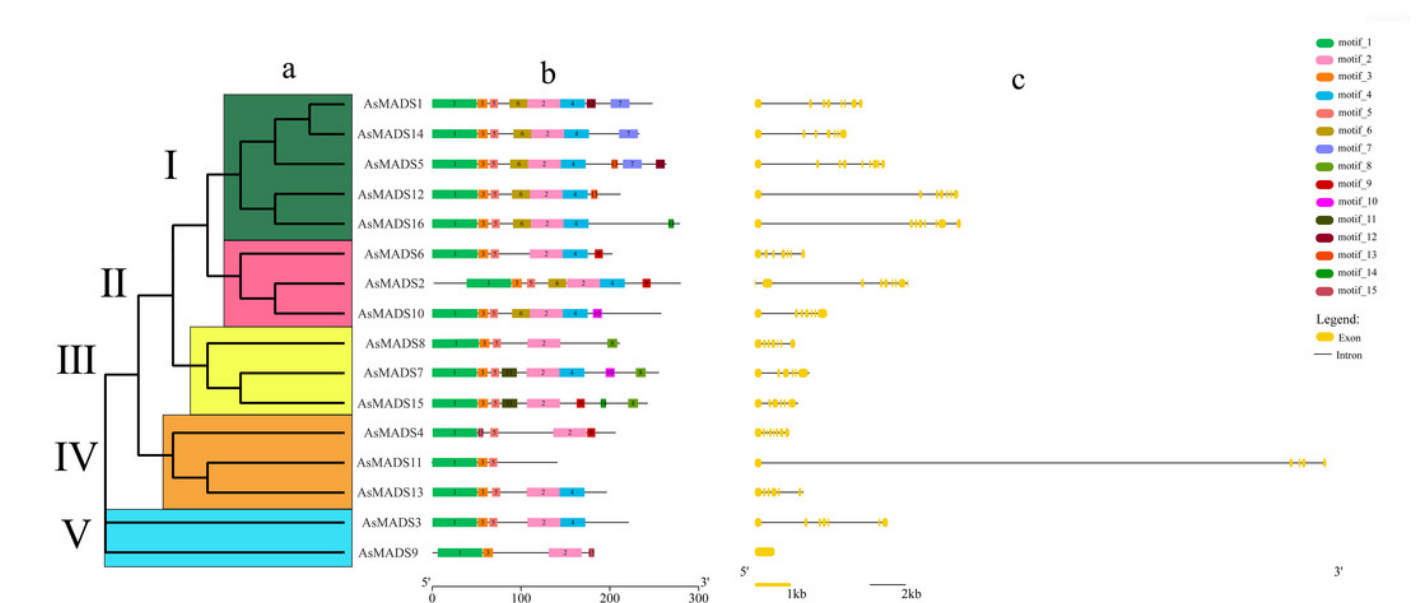


## Figure 4

Predicted three-dimensional domains of 16 AsMADS proteins from oat.

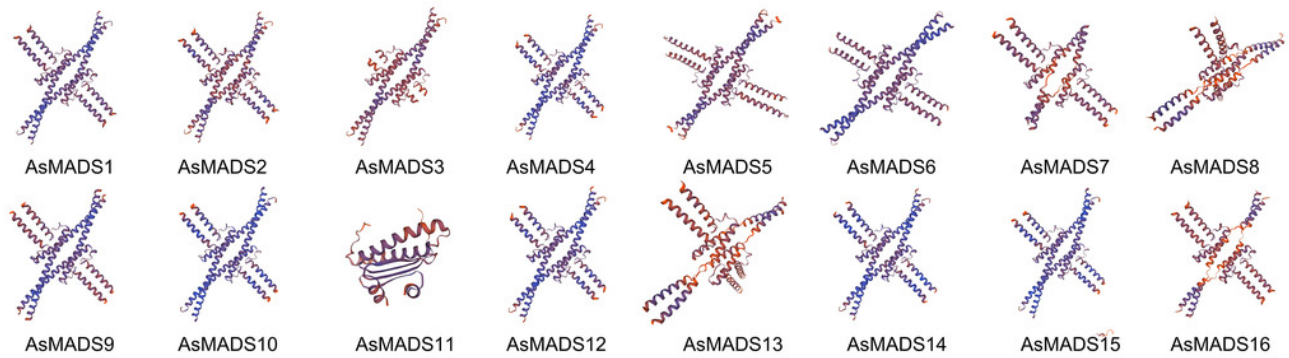


## Figure 5

Chromosomal location and collinearity analysis of 16 AsMADS genes.

(a) Chromosomal location of 16 AsMADS genes in oat. (b) Collinearity analysis of AsMADSs between oat, Arabidopsis, and rice. the Os, As and At respectively indicates that *Oryza sativa*, *Avena sativa*, *Arabidopsis thaliana*.

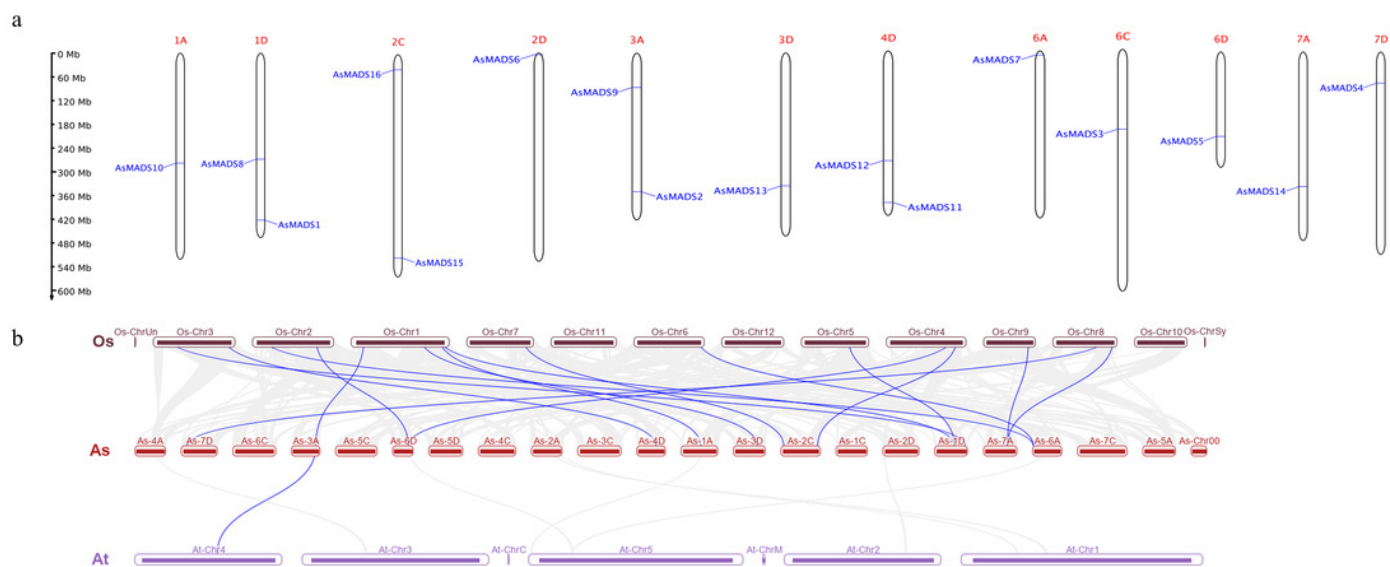


## Figure 6

Prediction of *cis*-elements in the 2k upstream regulatory regions of AsMADS genes.

Different colored boxes indicate different *cis*-elements.

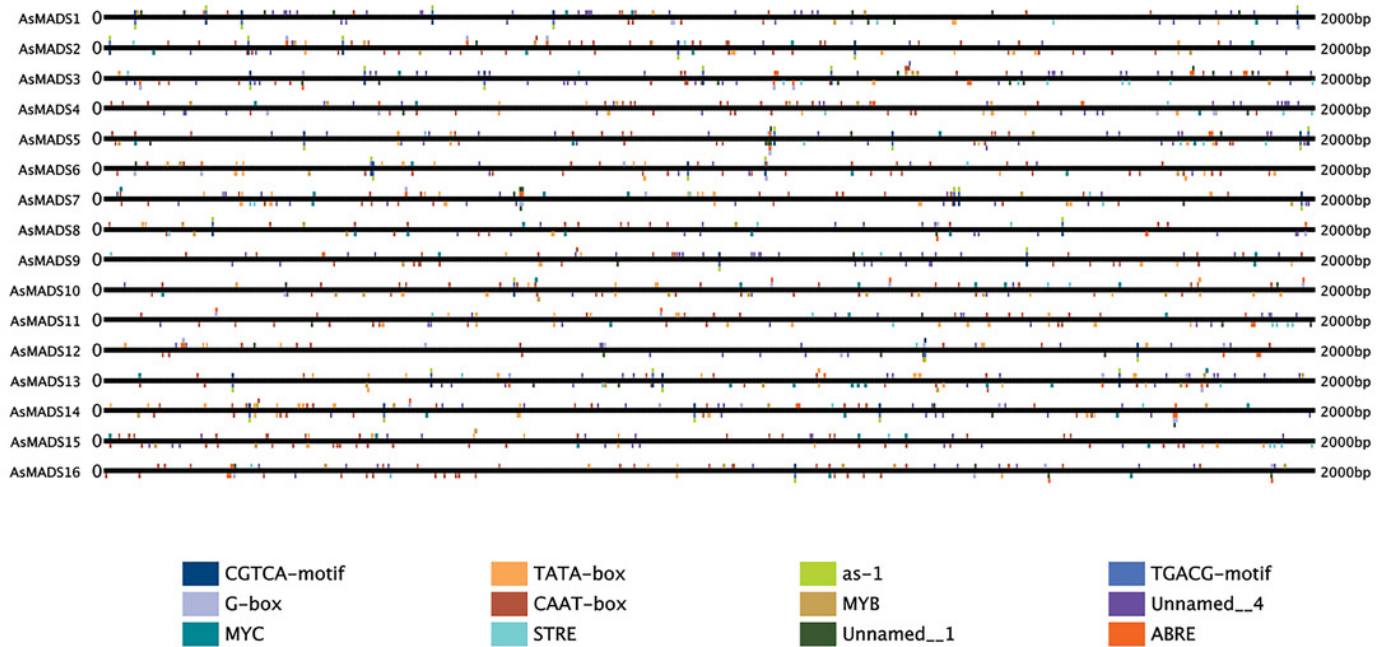


## Figure 7

Gene Ontology analysis of 10 AsMADS genes from RNA-seq data.

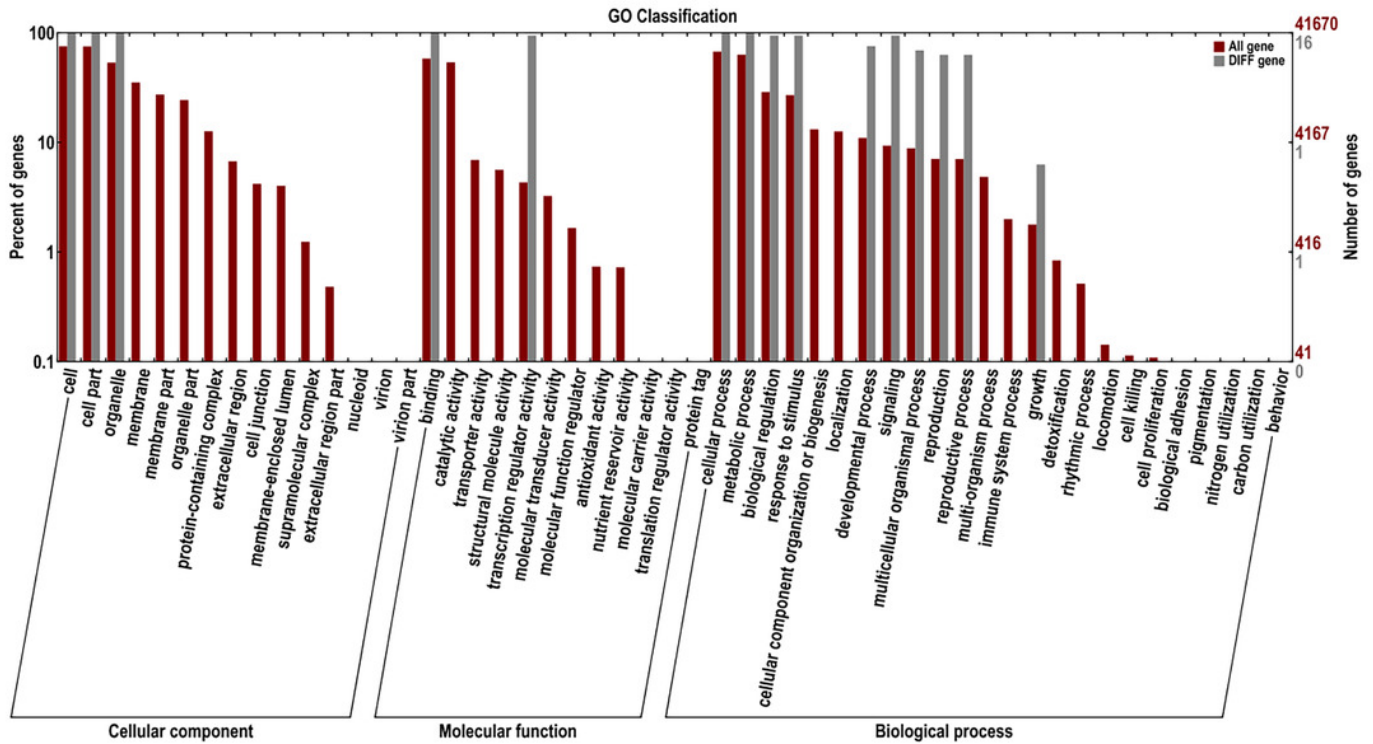


## Figure 8

Expression profiles analysis of 10 AsMADS genes from RNA-seq data.

Differentially expressed genes are screened in panicles (T01, T02, T07, and T08) and leaves (T03, T04, T05, and T06) at the oat initial differentiation stage of HQ2 and MSY4 under short-day conditions. Note: T0-T04 is HQ2. T05-T08 is MSY4. T01, T02, T07, and T08 is panicle. T03, T04, T05, and T06 is leaf.

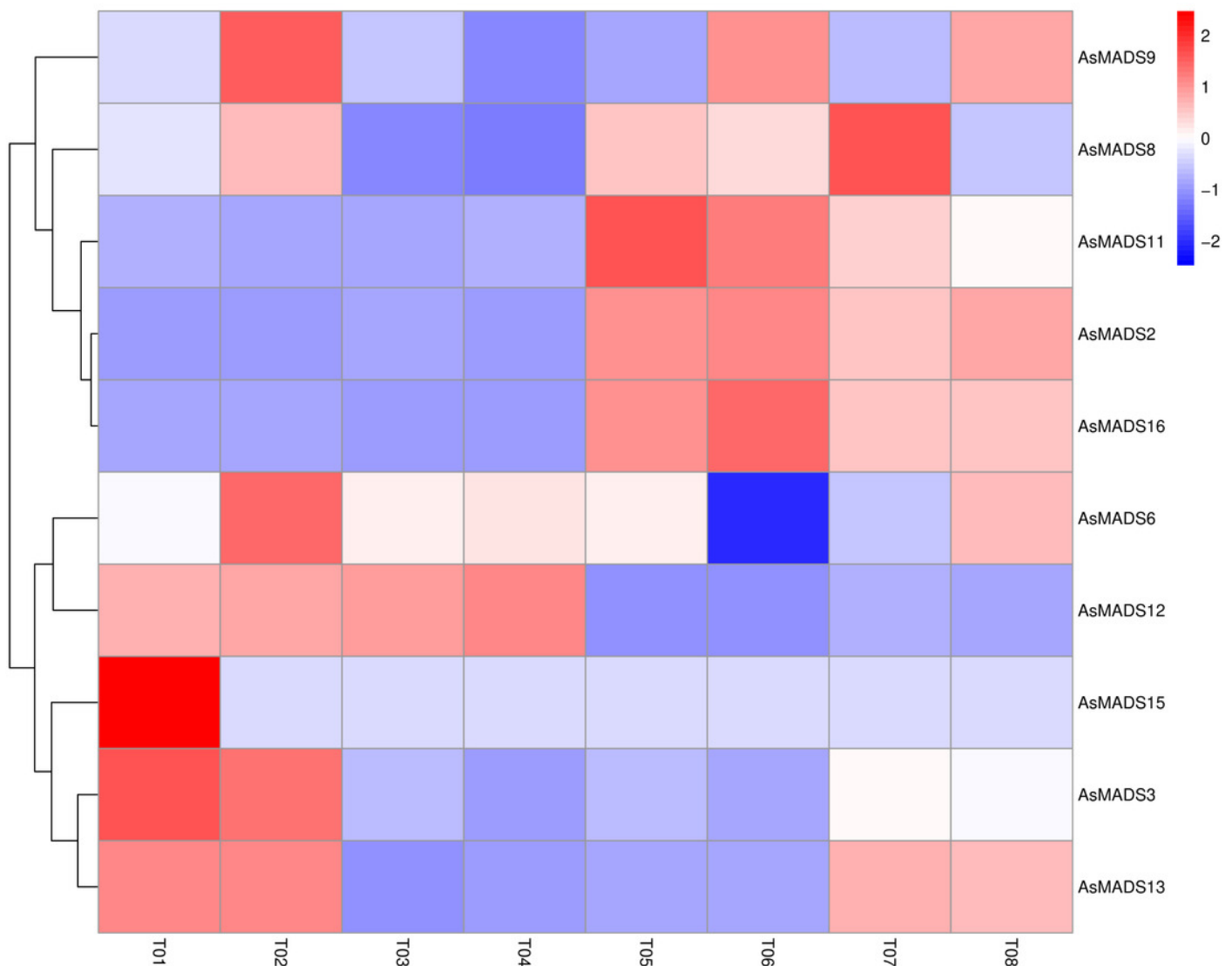


## Figure 9

Gene expression of 10 AsMADS genes in the initial stage, elongation stage and branch differentiation stage of HQ2 and MSY4 under short days from qPCR.

Note: qPCR data results of 10 AsMADS genes was normalized by z-score. Heatmap is performed in Metware cloud platform

tool(<https://cloud.metware.cn/#/tools/tool-form?toolId=168>). Each bar represents a gene. Red indicates that the gene is up-regulated, and blue indicates that the gene is down-regulated.

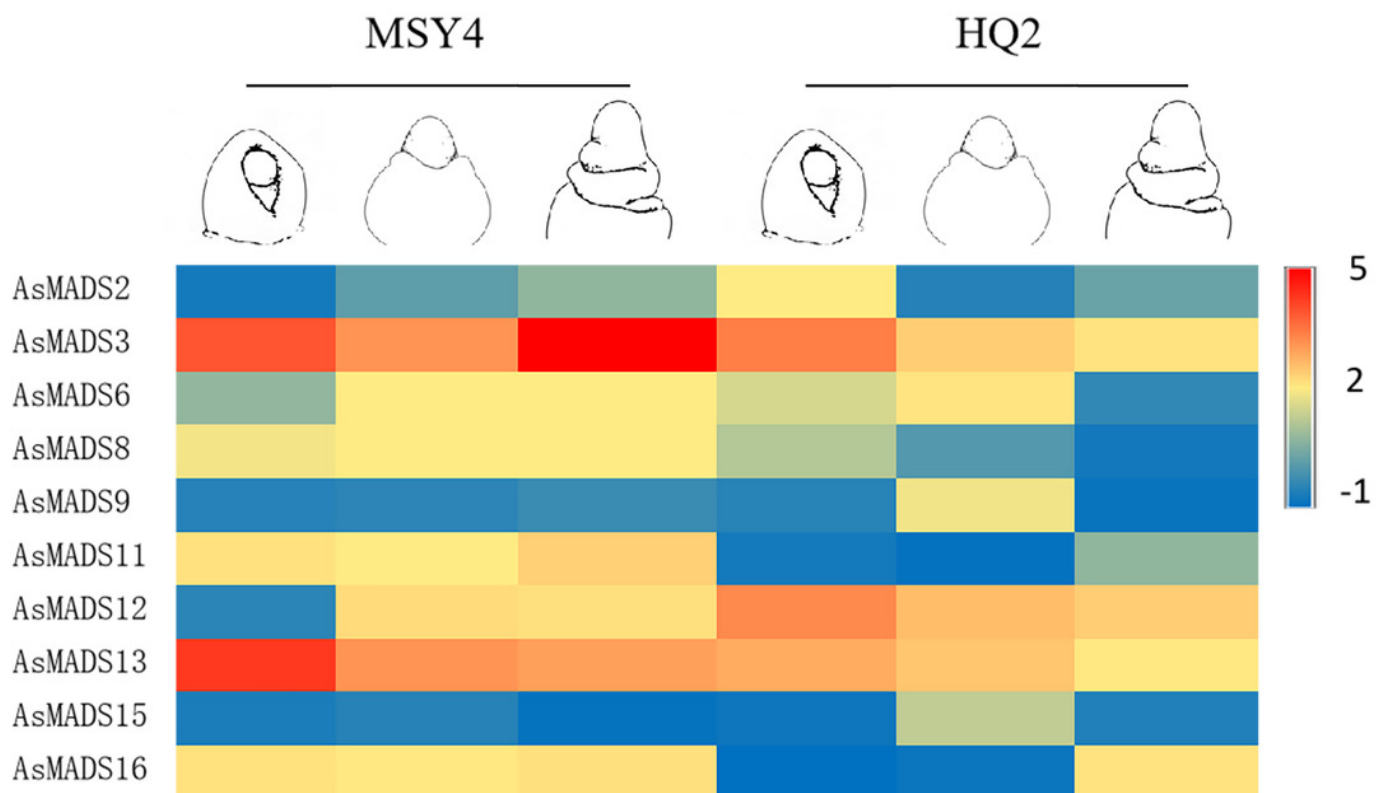


## Figure 10

Expression heat map of 10 AsMADS genes at different developmental stages of MSY4 under short days from qPCR.

Note: qPCR data results of 10 AsMADS genes was normalized by z-score. Heatmap is performed in Metware cloud platform

tool(<https://cloud.metware.cn/#/tools/tool-form?toolId=168>). Each bar represents a gene. Red indicates that the gene is up-regulated, and blue indicates that the gene is down-regulated.

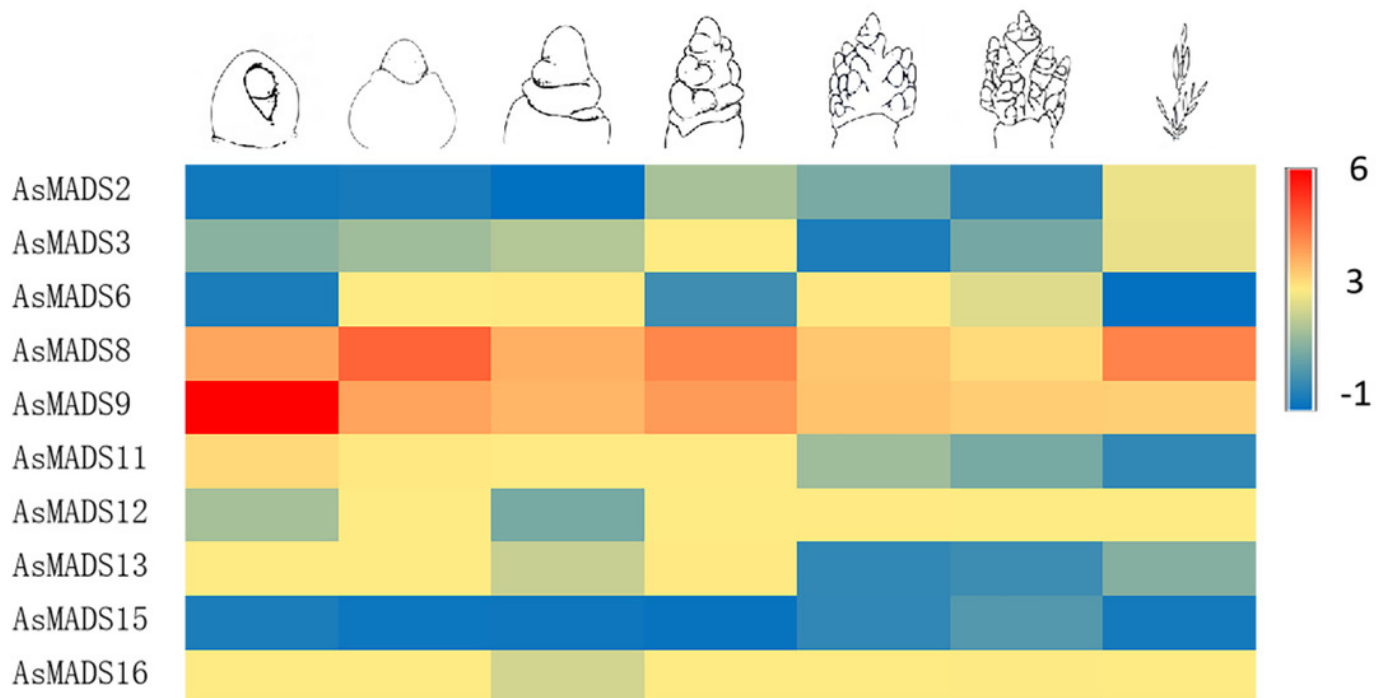


# Figure 11

Predicted photoperiodic pathway of MSY4 under short-day conditions.

Red boxes indicate up-regulation, blue boxes indicate down-regulation, yellow boxes indicate inconsistent expression patterns of multiple transcripts, and green boxes indicate unchanged expression levels

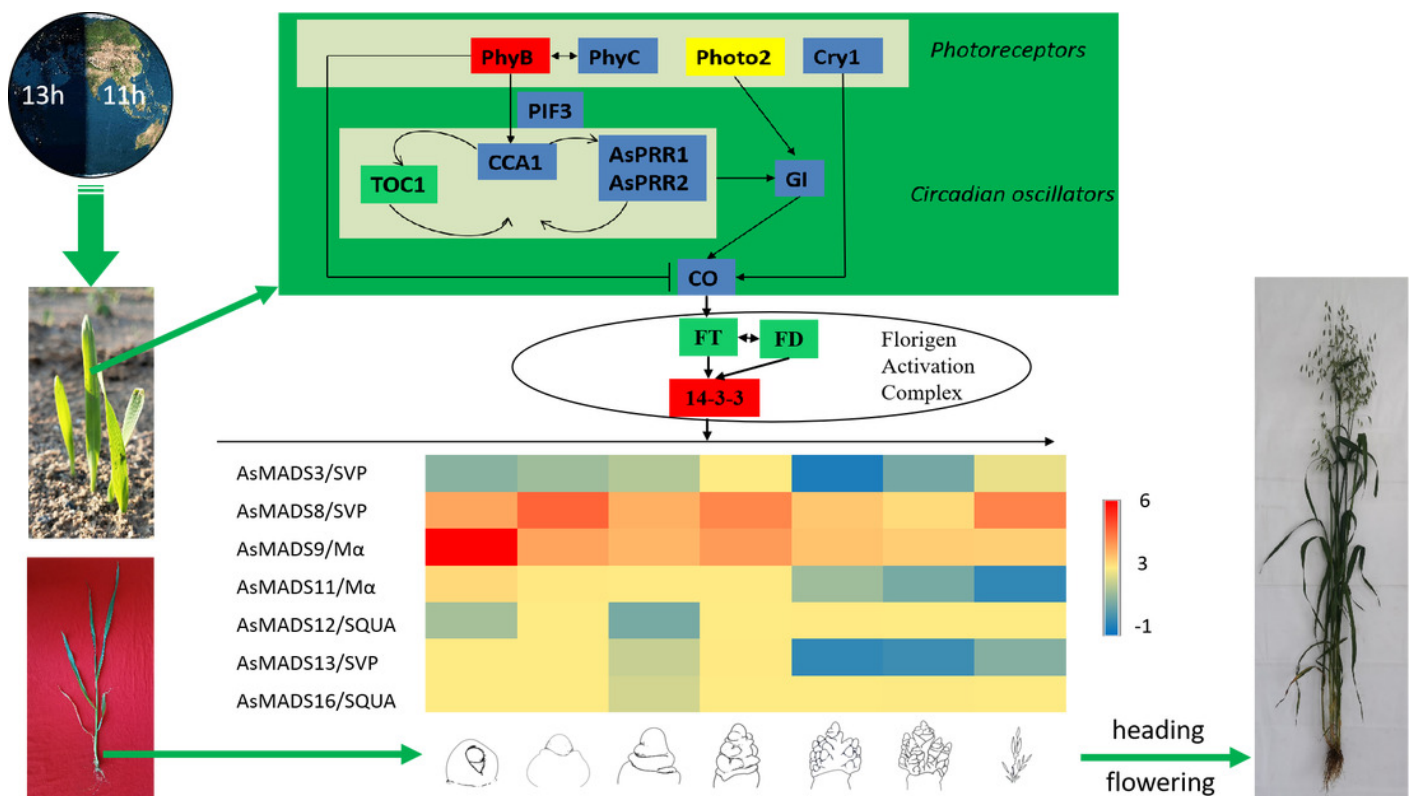


**Table 1** (on next page)

Information for the MADS gene family

1 Table 1:  
2 Information for the MADS gene family

Gene Name	Gene Id	Location	Size (AA)	Exon	Intron	Molecular Weight (KDa)	Isoelectric Points	Instability Index	GRAVY	Subcellular Location
AsMADS1	TRINITY_DN13687_c0_g2_i1.mrna1	1D:440731844-440737616	248	8	7	28.33	6.46	64.41	-0.797	Nuclear
AsMADS2	TRINITY_DN231_c1_g1_i5.mrna2	3A:354464249-354472711	278	10	9	31.61	9.01	54.8	-0.839	Nuclear
AsMADS3	TRINITY_DN32614_c0_g1_i3.mrna1	6C:205578143-205585989	221	7	6	24.64	5.52	49.5	-0.634	Nuclear
AsMADS4	TRINITY_DN3261_c0_g2_i2.mrna1	7D:80735581-80737035	206	8	7	23.77	7.02	62.67	-0.492	Nuclear
AsMADS5	TRINITY_DN3337_c0_g1_i3.mrna2	6D:221314556-221321673	263	9	8	29.83	8.9	45.02	-0.776	Nuclear
AsMADS6	TRINITY_DN3733_c0_g1_i1.mrna1	2D:4056942-4066252	202	7	6	23.43	8.8	60.05	-0.553	Nuclear
AsMADS7	TRINITY_DN383_c0_g1_i1.mrna1	6A:9765559-9768798	255	7	6	28.48	6.46	61.69	-0.515	Nuclear
AsMADS8	TRINITY_DN383_c1_g1_i2.mrna1	1D:279668871-279671412	209	7	6	24.33	9.08	64.25	-0.805	Nuclear
AsMADS9	TRINITY_DN39828_c0_g6_i1.mrna1	3A:87682568-87683651	182	1	0	20.14	6.76	54.46	-0.416	Nuclear
AsMADS10	TRINITY_DN4009_c0_g1_i6.mrna1	1A:289587547-289592225	257	7	6	28.69	9.15	60.67	-0.616	Nuclear
AsMADS11	TRINITY_DN42664_c0_g1_i9.mrna1	4D:391283530-391315386	142	5	4	16.11	9.09	65.59	-0.723	Nuclear
AsMADS12	TRINITY_DN6792_c2_g1_i3.mrna1	4D:282480902-282492339	211	7	6	24.63	9.25	60.9	-0.82	Nuclear
AsMADS13	TRINITY_DN6901_c0_g1_i1.mrna1	3D:340212580-340215197	196	7	6	22.32	8.67	44.82	-0.59	Nuclear
AsMADS14	TRINITY_DN695_c0_g1_i7.mrna1	7A:351371284-351376726	233	7	6	27.03	8.96	45.71	-0.845	Nuclear
AsMADS15	TRINITY_DN9392_c0_g1_i5.mrna2	2C:535820137-535822661	242	8	7	28.18	8.52	55.2	-0.558	Nuclear
AsMADS16	TRINITY_DN9814_c0_g1_i1.mrna2	2C:39788836-39799997	278	8	7	31.51	9.28	59.65	-0.856	Nuclear